Molecular dynamics simulation of clay hydration inhibition of deep shale

Zhang, Yayun; Xiao, Cong

DOI
10.3390/pr9061069

Publication date
2021

Document Version
Final published version

Published in
Processes

processes

MDPI

Article

Molecular Dynamics Simulation of Clay Hydration Inhibition of Deep Shale

Yayun Zhang [1,2] and Cong Xiao [3,*]

[1] State Key Laboratory of Shale Oil and Gas Enrichment Mechanisms and Effective Development, Beijing 100101, China; zhangyy.sripe@sinopec.com
[2] Sinopec Research Institute of Petroleum Engineering, Beijing 100101, China
[3] Delft Institute of Applied Mathematics, Delft University of Technology, Mekelweg 4, 2628 CD Delft, The Netherlands
* Correspondence: C.Xiao@tudelft.nl

Abstract: In the process of the exploitation of deep oil and gas resources, shale wellbore stability control faces great challenges under complex temperature and pressure conditions. It is difficult to reflect the micro mechanism and process of the action of inorganic salt on shale hydration with the traditional experimental evaluation technology on the macro effect of restraining shale hydration. Aiming at the characteristics of clay minerals of deep shale, the molecular dynamics models of four typical cations (K^+, NH_4^+, Cs^+ and Ca^{2+}) inhibiting the hydration of clay minerals have been established by the use of the molecular dynamics simulation method. Moreover, the micro dynamics mechanism of typical inorganic cations inhibiting the hydration of clay minerals has been systematically evaluated, as has the law of cation hydration inhibition performance in response to temperature, pressure and ion type. The research indicates that the cations can promote the contraction of interlayer spacing, compress fluid intrusion channels, reduce the intrusion ability of water molecules, increase the negative charge balance ability and reduce the interlayer electrostatic repulsion force. With the increase in temperature, the inhibition of the cations on montmorillonite hydration is weakened, while the effect of pressure is opposite. Through the molecular dynamics simulation under different temperatures and pressures, we can systematically understand the microcosmic dynamics mechanism of restraining the hydration of clay in deep shale and provide theoretical guidance for the microcosmic control of clay hydration.

Keywords: deep shale; clay mineral; inorganic cation; chemical inhibition; molecular dynamic simulation

Citation: Zhang, Y.; Xiao, C. Molecular Dynamics Simulation of Clay Hydration Inhibition of Deep Shale. *Processes* **2021**, *9*, 1069. https://doi.org/10.3390/pr9061069

Academic Editor: Andrew S. Paluch

Received: 18 May 2021
Accepted: 17 June 2021
Published: 19 June 2021

1. Introduction

With the continuous exploitation of shale gas, the drilling depth is gradually increasing worldwide, and deep shale gas resources have gradually become the focus of the oil and gas industry. Meanwhile, with the high-temperature and high-stress environment, the wellbore collapse of deep shale becomes increasingly serious, i.e., more sudden and destructive, and the sloughing is more severe. Clay minerals are one of the main mineral components of shale. The hydration of clay minerals is one of the main causes of wellbore collapse [1,2]. With the increase in buried depth, the temperature and pressure environment of deep shale will gradually increase. The deterioration of the hydration of clay minerals under high temperature and high pressure is the key factor leading to wellbore collapse of deep shale [3]. Therefore, fully understanding the mechanism of clay hydration expansion and chemical inhibition is of great strategic significance to realize macro and micro control of deep shale hydration, maintain wellbore instability and ensure economic and effective development of shale gas.

There are two kinds of traditional methods for researching the inhibition mechanism of clay mineral hydration [4,5]. The first is the theoretical analysis based on physical chemistry theory, in which the main understanding is that the mosaic effect of K^+ and

NH_4^+ ions on the clay minerals surface fixes the crystal lattice, the surface adsorption of various kinds of inhibitory ions tightens the crystal layer and cationic and surfactant polar groups compress the electric double layer and reduce the charge repulsion between layers. However, the above theoretical analysis is difficult to be verified by experiments and is not intuitive. The second is the experimental characterization methods, mainly including XRD layer spacing, zeta potential, capillary suction timer (CST), cation exchange capacity (CEC) and linear expansion and rolling recovery, as well as various mechanical and chemical coupling macro and micro experimental methods. However, at present, various laboratory test methods are indirect evaluation methods, which characterize the results of inhibitor action. In general, the traditional evaluation methods of the clay hydration inhibition have difficulty in tracking and characterizing the micro process of the inhibitor exerting the chemical inhibition effect in real time, and they ignore the micro dynamic mechanism of the chemical inhibition effect of various treatment agents at the micro-nanoscale on clay hydration. However, the molecular simulation method can obtain the macroscopic properties of the system through atomic-scale simulation, which is widely used in the analysis of hydration mechanism and hydration inhibition process of clay minerals.

With the use of Monte Carlo (MC) and molecular dynamics (MD) methods, the hydration characteristics of different montmorillonite (MMT) models (Na-MMT, Mg-MMT) were analyzed, and the applicability of different water molecular models in clay hydration simulation was studied [6–8]. E.S. Boek et al. [9] quantitatively explained the difference in swelling characteristics between Na-MMT and K-MMT and qualitatively analyzed the inhibition mechanism of organic molecules to the clay hydration with the help of grand canonical Monte Carlo (GCMC) and molecular dynamic (MD) methods. They found that PEG molecules can weaken the hydration swelling of clay by affecting the desorption of water molecules. Sposito et al. [10–12] researched the structural characteristics of Li-MMT, Na-MMT and K-MMT hydration through MC methods. Ruth M. Tinnach et al. [13] investigated the diffusion and adsorption behavior of water molecules and ions (Br^- and Ca^{2+}) in montmorillonite by molecular dynamics simulation and predicted the average density of ions and water in the clay interlayer region. Laura N. Lammers et al. [14] analyzed the competitive adsorption of Cs and Na at different sites of illite (edge, basal plane and interlayer) by atomic simulation. The hydration characteristics of Na-MMT, K-MMT and Ca-MMT were investigated by MC simulations at higher pressures and temperatures [15]. With the use of MC and MD simulations, the distribution behavior of water molecules and cations in the interlayer region was analyzed [16–19], and the effect of inorganic salts on the mechanical properties of MMT was explored. Anderson et al. [20] investigated the interaction of poly(propylene oxide) diamine, poly(ethylene glycol) and poly(ethylene oxide) diacrylate inhibitor molecules with MMT at 300 K. Zhang et al. [21] used MD simulation to study the structure and dynamic characteristics of water molecules, Na^+ and poly(ethylene glycol) (PEG) in the interlayer region of Na-MMT. They found that different PEG molecules exhibit distinct performances in the MMT interlayer. The existence of PEG reduced the mobility of water and counterions, and the formation of the Na^+-PEG complex reduced the hydration of Na^+. In general, previous reports mainly focused on the structure and dynamic behavior of water and cations in the clay mineral hydration process and partially revealed the inhibition mechanism of clay hydration expansion. However, the microstructure and dynamic response characteristics of the chemical inhibition process of different inhibitory ions were not revealed, and the laws of the chemical inhibition response to different temperatures, pressures, ion types and concentrations were not fully understood.

In this paper, based on MD simulation method, according to the characteristics of typical clay minerals contained in deep shale, combined with the types of inorganic salinization inhibitors commonly used in the field, the molecular dynamics models for micro inhibition evaluation of four typical cations (K^+, NH_4^+, Cs^+ and Ca^{2+}) inhibiting clay hydration were established. The MD simulations of inhibiting hydration of clay minerals under different temperatures and pressures, types and concentrations of cation ions were carried out. Then,

the micro mechanism of chemical inhibition effect of typical inorganic salt inhibitors on clay hydration and the temperature and pressure response characteristics were analyzed systematically and deeply.

2. Molecular Dynamics Simulation of Clay Hydration Inhibition

2.1. Simulation Scheme

In this paper, molecular dynamics models of typical montmorillonite systems with different interlayer particles (water molecules and inorganic salts) were established, and 72 groups of cationic hydration inhibition molecular dynamics simulations were carried out under different temperature (25, 75, 125 and 150 °C) and pressure (0.1, 30, 60 and 90 MPa) conditions, which can be divided into two modes.

The simulation scheme of mode 1 is shown in Table 1. In mode 1, at 25 °C and 0.1 MPa, two systems of Mg-substituted montmorillonite (Mg-Sub-MMT) and Fe-substituted montmorillonite (Fe-Sub-MMT) were used to carry out eight sets of molecular simulations of hydration inhibition. The interlayer domain of montmorillonite contains 72 water molecules and six electric charges of K^+, NH_4^+, Cs^+ and Ca^{2+}, which represents the formation of two-layer water molecular film and the replacement of interlayer exchangeable sodium ions.

Table 1. Mode 1: Simulation scheme for changing the exchangeable cationic.

	Systems		**Interlayer Particles**	
Mode 1	Mg-Sub-MMT Fe-Sub-MMT	25 °C 0.1 MPa	6 K^+ 6 NH_4^+ 6 Cs^+ 3 Ca^{2+}	72 water molecules

The simulation scheme of mode 2 is shown in Table 2. In model 2, there are 72 water molecules in the interlayer domain, and the equilibrium cations are the same as the six Na^+ ions in the original model, but four kinds of inhibitory cations enter the interlayer domain in the form of saturated inorganic salt solution. At the same time, eight kinds of temperature and pressure conditions were set, including four conditions with constant temperature and variable pressure and four conditions with constant pressure and variable temperature, and 64 groups of inhibitory MD simulations were carried out. The scheme of mode 2 has two objectives: one is to compare the inhibition differences of different types of cations, and the other is to study the temperature and pressure response law of hydration inhibition of different cations.

Table 2. Mode 2: Simulation scheme for changes of saturated inorganic salts under temperature and pressure conditions construction.

	Systems					**Interlayer Particles**	
Mode 2	Mg-Sub-MMT	Constant temperature (25 °C) and variable pressure 0.1	30	60	90	Saturated KCl solution Saturated NH_4Cl solution	72 water molecules + 6Na^+
	Fe-Sub-MMT	Constant pressure (60 MPa) and variable temperature 25 °C	75 °C	125 °C	150 °C	Saturated CsCl solution Saturated $CaCl_2$ solution	

2.2. Model Construction

Montmorillonite (MMT) is a clay mineral composed of 2:1 phyllosilicate layers; that is, an alumina (Al_2O_3) octahedral (O) layer is sandwiched between two silica (SiO_2) tetrahedral (T) layers. Due to the existence of isomorphic substitution, MMT is usually negatively charged. Mg^{2+}, Fe^{2+} or Fe^{3+} in the octahedral layer is more likely to substitute Al^{3+}. However, the substitution of Al^{3+} to Si^{4+} in the tetrahedral layer is relatively rare. In this paper, the Mg-substituted montmorillonite model (Mg-Sub-MMT) and Fe-substituted montmorillonite model (Fe-Sub-MMT) in which Fe^{2+}/Mg^{2+} replace Al^{3+} in the octahedron

were established. The clay structures refer to the Wyoming MMT model, whose unit cell formula is $Na_{0.75}(Si_{7.75}Al_{0.25})(Al_{3.5}M_{0.5})O_{20}(OH)_4$, where M represents the substitutional cation (Mg^{2+} and Fe^{2+}). The layer charge of lattice substitution in the supercell is −0.75/cell, which is balanced by interlayer cation Na^+.

Firstly, the Mg-Sub-MMT and Fe-Sub-MMT supercell structures were constructed. Then, based on the Metropolis Monte Carlo algorithm, water molecules were added into the interlayer for the construction of the Mg-Sub-MMT and Fe-Sub-MMT hydration model with two layers of water molecules. In mode 1, all interlayer Na^+ was replaced by equal charge of inhibitory cations, and the established model with inhibitory cations as equilibrium cations is shown in Figure 1 below.

In mode 2, the corresponding saturated concentration of inhibitory inorganic salt ions was added to the model, and the hydration model of montmorillonite with saturated concentration of inorganic salt solution in the interlayer domain was established, as shown in Figure 2 below (only the Mg-Sub-MMT model is shown).

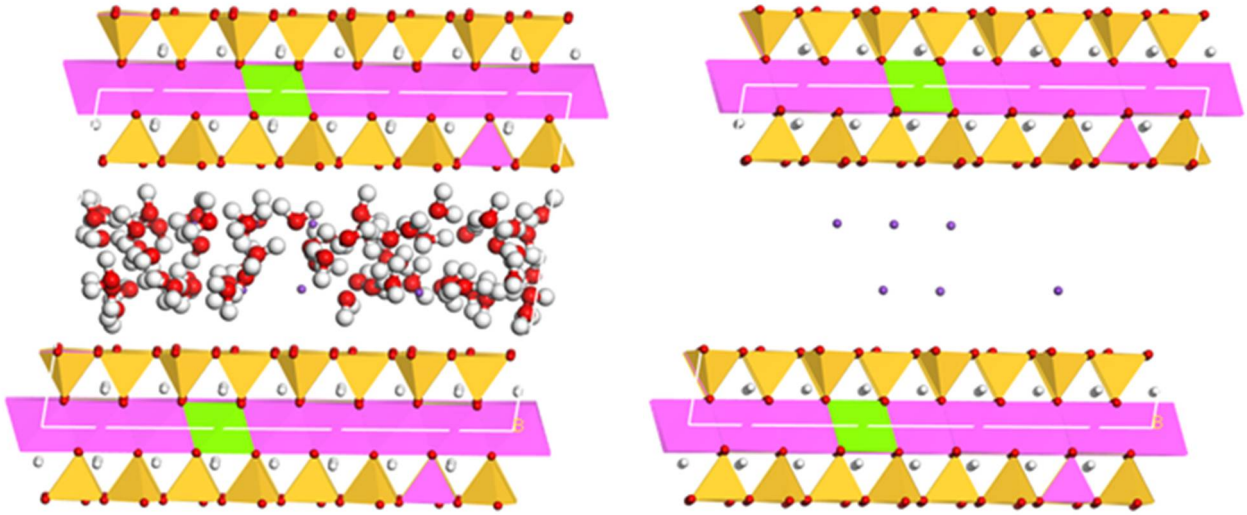

(**a**) 72-K-Mg-Sub-MMT

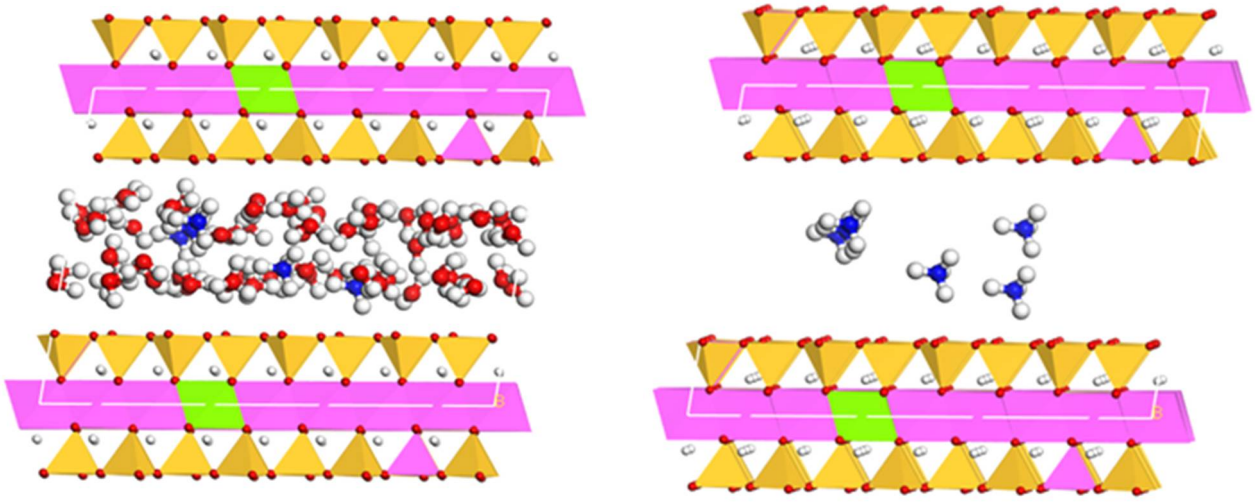

(**b**) 72-NH_4-Mg-Sub-MMT

Figure 1. *Cont.*

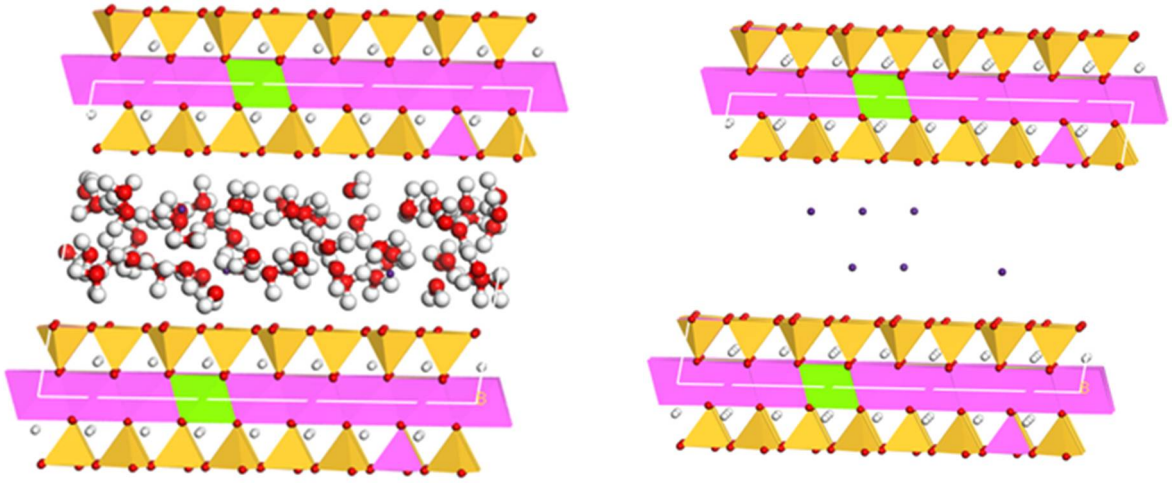

(**c**) 72-Cs-Mg-Sub-MMT

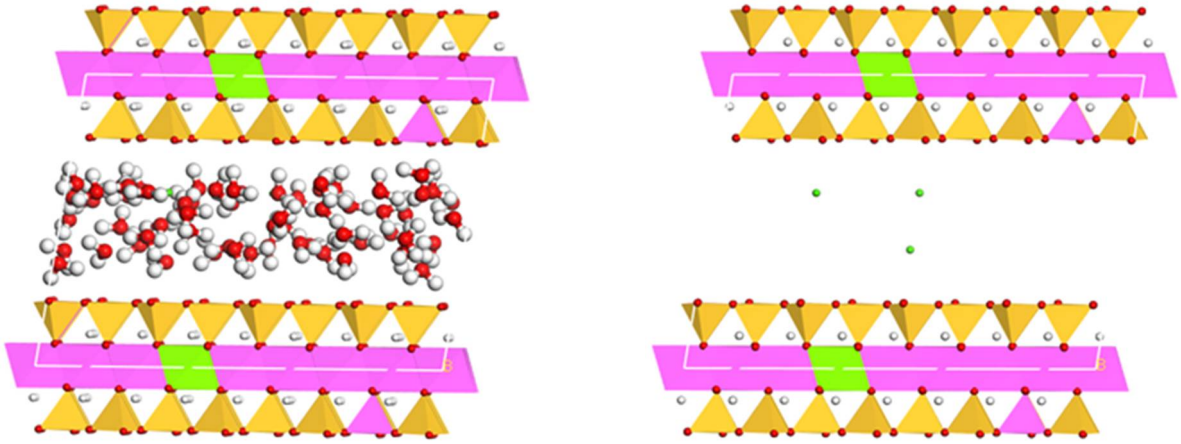

(**d**) 72-Ca-Mg-Sub-MMT

Figure 1. Initial structure of Mg-Sub-MMT with inhibitory cations as counterions. The water molecules in the interlayer are not shown in the right images of different models. The color coding for the atoms is H, white; O, red; Mg, green; Al, pink; Si, gold; K, violet; N, blue; Cs, deep purple; Ca, yellow-green.

2.3. Simulation Details

Clayff is a special clay mineral force field simulation [22]. Considering that there is no force field information used to describe N element in Clayff, universal force field (UFF) [23–25] was used in the simulation system involving NH_4^+, and Clayff was still used in other simulations. Although the accuracy of UFF force field simulation of clay minerals is not as good as Clayff force field, it is also one of the force fields often used by predecessors in the simulation of clay minerals and the simulation accuracy can meet the requirements.

UFF force field is a universal force field. The element types cover the whole periodic table of elements, but only diagonal terms and simple harmonic functions are used. The function form is simple, and the parameters are mostly obtained by experimental fitting. QEQ algorithm is used by default for partial charge calculation.

The geometry of the MMT model was optimized by the smart minimizer algorithm. The long-range Coulombic interaction was calculated using the Ewald summation method. Each configuration was relaxed in NVT assemblage with Materials Studio (MS) through five decreasing temperature stages with a time step of 0.50 fs. Then, dynamic simulations

under different temperature and pressure conditions were carried out in the NPT ensemble for 1000 ps. Periodic boundary conditions were used to avoid interface effects.

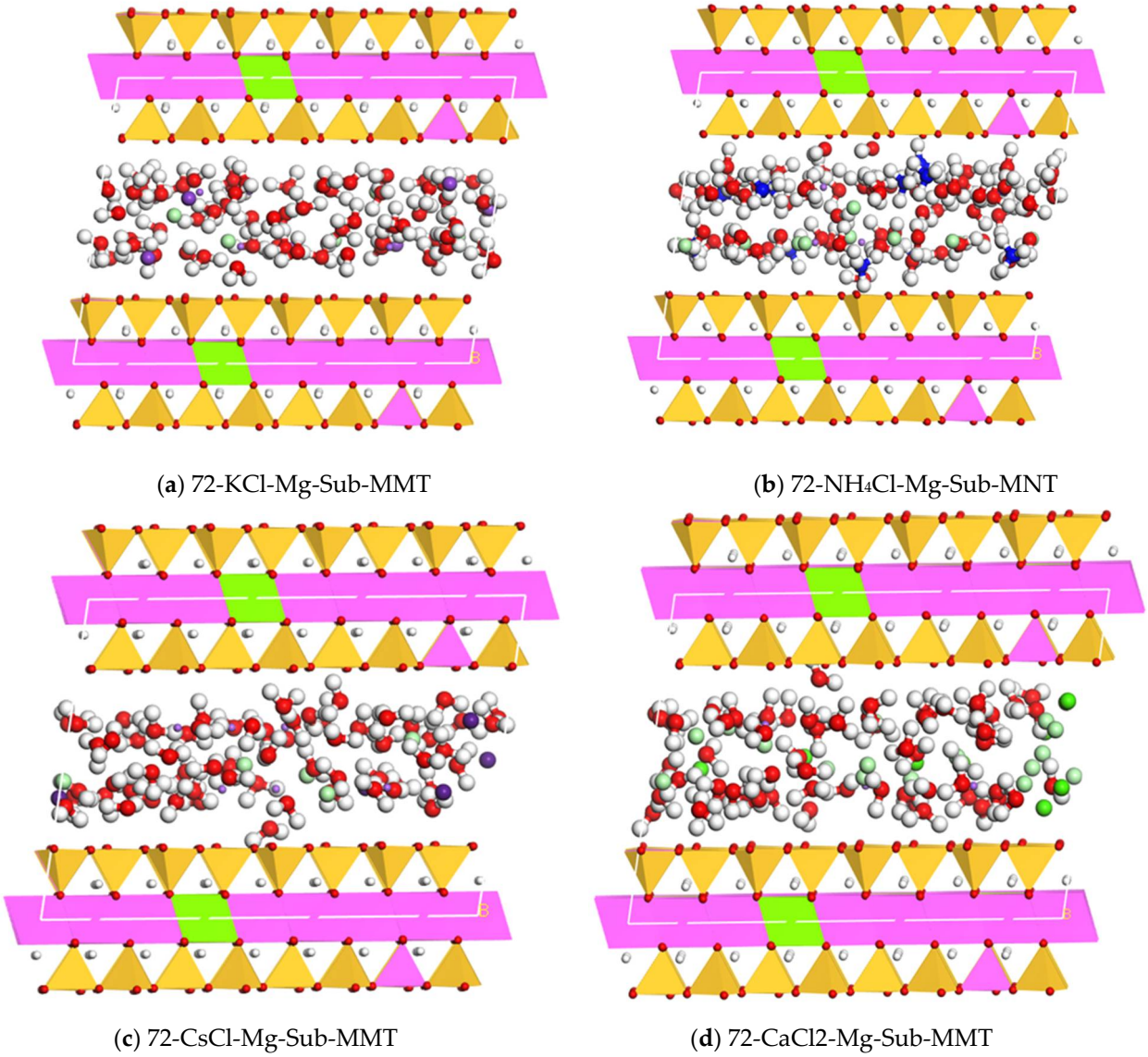

(**a**) 72-KCl-Mg-Sub-MMT (**b**) 72-NH_4Cl-Mg-Sub-MNT

(**c**) 72-CsCl-Mg-Sub-MMT (**d**) 72-CaCl2-Mg-Sub-MMT

Figure 2. Initial structure of Mg-Sub-MMT with saturated salt solution. The color coding for the atoms is H, white; O, red; Mg, green; Al, pink; Si, gold; K, violet; N, blue; Cs, deep purple; Ca, yellow-green; Cl, lavender.

3. Results

3.1. Micro Mechanism of Cationic Clay Hydration Inhibition

In this study, by comparing the hydration characteristics of water molecules and cations after cations enter the interlayer region, the micro mechanism of hydration inhibition effect of representative cations was investigated.

3.1.1. Interlayer Spacing

The interlayer spacing of the two substituted MMT systems under different inhibitory cations is shown in Table 3. The simulation results of various inhibitory cation systems in this paper are very close to those of previous similar systems, and the slight difference is probably caused by the difference in the number of double-layer water molecules and the force field and ensemble used in previous simulation work.

Table 3. Interlayer spacing of MMT under different inhibitory cations.

Interlayer Spacing (Å)		This Paper		Comparative Literature	
		Mg-Sub-MMT	Fe-Sub-MMT	Molecular Simulation	Experiment
Na^+	72 water molecules	14.92	14.89	14.7 [26] 14.96 [27] 15.28 [8]	14.7 [28] 15.4 [29]
K^+		14.45	14.79	14.31 [30] 15.89–16.83 [31]	15.6 [32]
NH_4^+		14.75	14.85	-	-
Cs^+		14.89	14.92	14.88 [30] 15.13 [33]	-
Ca^{2+}		15.07	15.31	14.6 [30] 14.73 [33]	15.55 [34]

Through the comparison of the simulation results, it can be found that after adding different inhibitory cations, the interlayer spacing of the two substituted montmorillonite systems is significantly different. Under the conditions of K^+, NH_4^+ and Cs^+, the interlayer spacing of the two substituted montmorillonite systems is significantly reduced, indicating that these three ions can inhibit the expansion of the montmorillonite crystal layer and promote the contraction of the crystal layer, but the degree of influence is different. The order of inhibition ability of interlayer expansion is $K^+ > NH_4^+ > Cs^+$. As for Ca^{2+}, the interlayer spacing of the two substituted montmorillonite systems increases slightly, and the increase is more obvious in the Fe-Sub-MMT, which shows that calcium ion has difficulty in effectively inhibiting the expansion of the MMT crystal layer.

3.1.2. Distribution of Water Molecules and Ions

The relative concentration distribution characteristics of water molecules and cations in the interlayer region after the equilibrium of the hydration inhibition dynamics simulation in Mode 1 are shown in Figures 3 and 4 below.

The relative concentration distribution curve of water molecules showed that the distribution characteristics of water molecules in the interlayer domain did not change significantly under different inhibitory cations (except NH_4^+), and a relatively stable two-layer water molecular film would be formed. Although the two-layer water molecular film can still be formed in the system with NH_4^+ as the counterions, the concentration curve fluctuates slightly and the peak shape splits, which indicates that the arrangement of the water molecular film in the interlayer becomes not tight at this time, because the addition of NH_4^+ has a certain destructive effect on the hydrogen bond between water molecules in the two-layer water molecular film.

As shown in Figure 4, when the inhibitory cations enter the interlayer domain, the peak values of the relative concentration distribution curve of cations in the interlayer domain are closer to the silica surface of the montmorillonite tetrahedral layer than those of the noninhibitory sodium ions. In addition to calcium ions, the distributions of the other three ions in the interlayer domain all showed multimodal properties. Similar to the sodium ion, the calcium ion tends to be far away from the surface of montmorillonite tetrahedron under the condition of 72 water molecules (that is, under the condition of double water molecules) and distributes in the middle of the interlayer domain. Combining with more water molecules, it forms an outer spherical coordination structure. The relative concentration distribution curve shows a strong single peak, and it is more prominent in the Fe-Sub-MMT system. K^+, NH_4^+ and Cs^+ show obvious multipeak properties in the interlayer domain and are closer to the silica surface, indicating that the three ions are more easily adsorbed by the clay mineral surface than Na^+. However, their distribution in the interlayer domain of montmorillonite crystal is not symmetrical, and some peaks are always inclined to one side of the silica surface, which is more obvious in the Fe-Sub-MMT system.

3.1.3. Conduction of Ions and Water Molecules

The diffusion coefficients of ions and water molecules in the interlayer domain of the two montmorillonite systems are shown in Figure 5 below. Compared with the Na^+ system, the diffusion coefficient of interlayer water can be reduced to some extent by adding four kinds of inhibitory cations, but the influence degree of each ion is quite different. The most

significant decrease in diffusion ability is in the Ca^{2+} system, followed by Cs^+, NH_4^+ and K^+. This is because the hydration radius and coordination number of Ca^{2+} are the largest, and more interlayer water molecules are combined to occupy the diffusion channels in the interlayer domain, which leads to the most significant decrease in the diffusion ability of water molecules in the Ca^{2+} system. Moreover, it can be observed that the inhibitory cations have the same effect in the two substitution models, and the diffusion ability of the Mg-Sub-MMT system decreases slightly (35% on average). On the other hand, the diffusion ability of the four inhibitory cations in the interlayer domain changed significantly. Under the condition of the same water content (fixed 72 water molecules), except for calcium ions, the interlayer diffusion ability of the three inhibitory cations is greater than that of sodium ion, and the order of diffusion ability is $NH_4^+ > K^+ > Cs^+ > Na^+$. According to the simulation of cation diffusion in pure water, when the amount of charge is the same, the diffusion ability of ions is inversely proportional to the radius of ions. The order of ion radius is $Cs^+ > K^+ > NH_4^+ > Na^+$, so the diffusion ability of the four ions in pure water is $Cs^+ < K^+ < NH_4^+ < Na^+$. Obviously, in the interlayer domain of montmorillonite, the diffusion ability of these monovalent ions is quite different from that in pure water, which indicates that the diffusion process of cations in the interlayer domain is significantly affected by clay wafer.

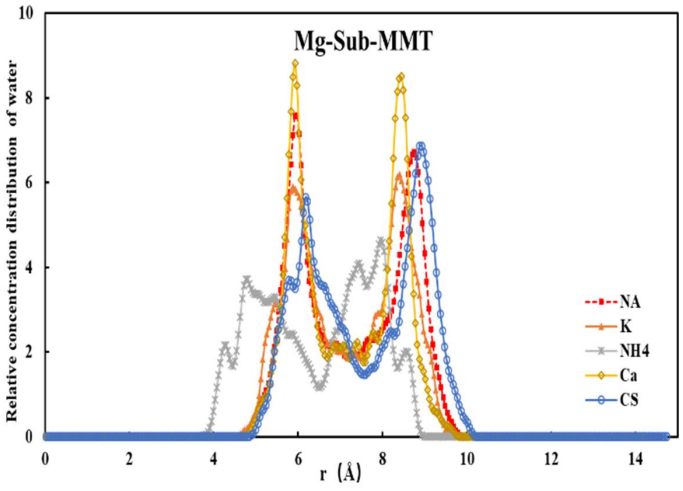

(**a**) Mg-Sub-MMT

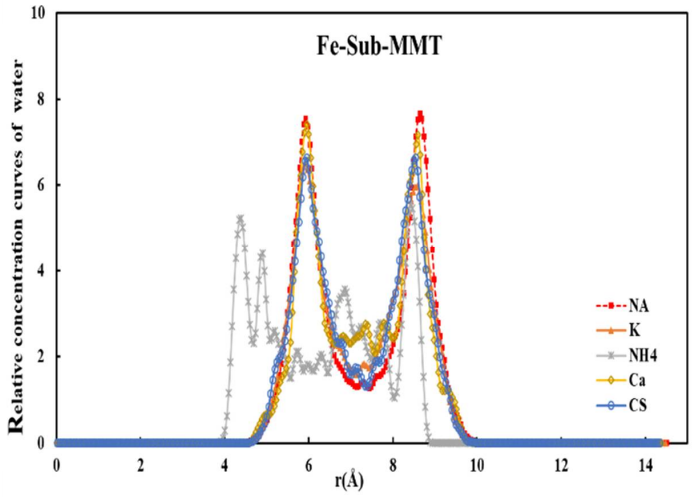

(**b**) Fe-Sub-MMT

Figure 3. Z-axis relative concentration curves of water.

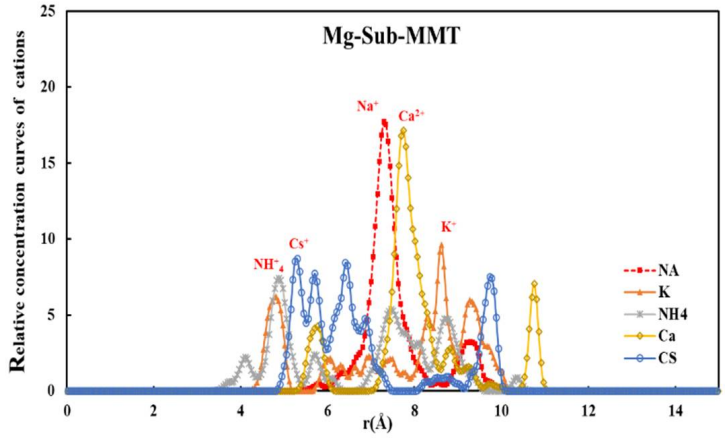

(**a**) Mg-Sub-MMT

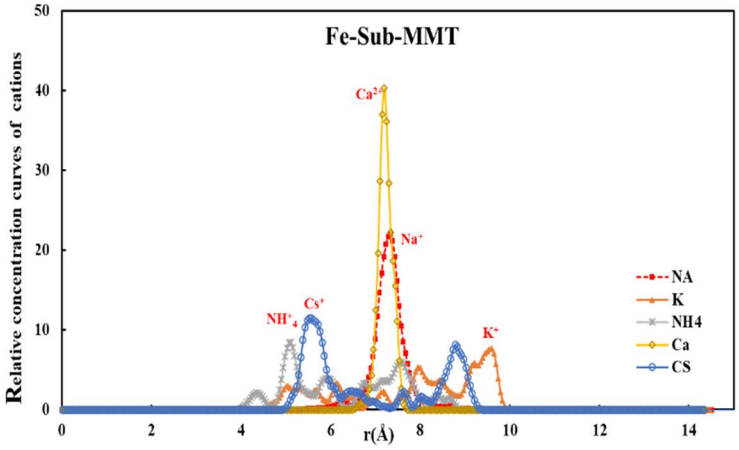

(**b**) Fe-Sub-MMT

Figure 4. Z-axis relative concentration curves of counterion.

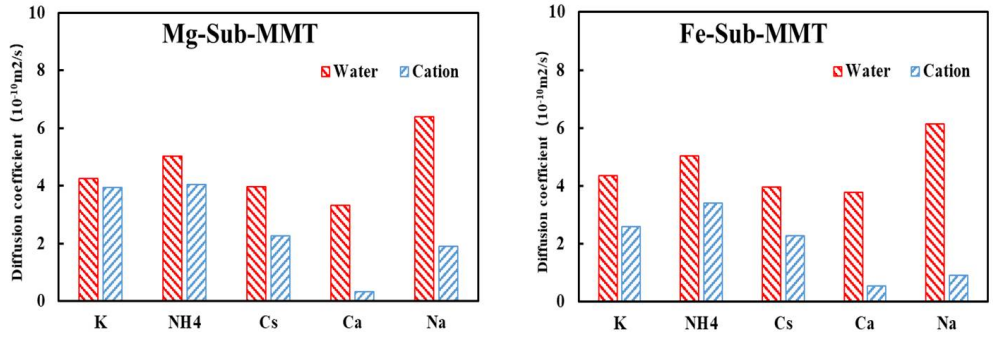

(**a**) Mg-Sub-MMT (**b**) Fe-Sub-MMT

Figure 5. Diffusion coefficient of counterions and water in different MMT systems.

3.2. Response of Cationic Clay Hydration Inhibition to Temperature and Pressure

In mode 2, with temperature rising, the diffusion performance of water molecules after adding saturated inorganic salt solution in the interlayer domain was determined, as shown in Figure 6 below. It can be found that the water diffusivity still increases significantly with the increase in temperature after adding saturated inhibitory inorganic salt solution at different temperatures. The results show that the addition of cations inhibits the water diffusivity in the interlayer domain but does not change the overall trend of temperature

promoting the invasion of water molecules into the interlayer domain. However, compared with the Na^+ system without inhibitory salt solution at the same temperature and pressure, the diffusion coefficient of water molecules decreases in varying degrees after adding salt solution. This shows that the degree of inhibition of the saturated inhibitory salt solution on the diffusion of water molecules in the interlayer decreases with the increase in temperature. For example, in the Mg-Sub-MMT system with saturated KCl solution, the water molecule diffusion coefficient is 2.41 $\times$ 10^{-10} m^2/s at 25 °C and 60 MPa. However, the water diffusivity in the Mg-Sub-MMT system without adding inhibitory solution is 3.59 $\times$ 10^{-10} m^2/s. That is, the reduction in the diffusion coefficient of the inhibitor to water molecules is 32.97%. However, at 150 °C and 60 MPa, the diffusion coefficient of water molecules decreases from 21.51 $\times$ 10^{-10} to 13.46 $\times$ 10^{-10} m^2/s. The degree of reduction is 21.51%. Comparing the four kinds of inhibitory salt solutions, it is found that the average degree of inhibition of the saturated $CaCl_2$ solution on the diffusion ability of water molecules is the largest, followed by CsCl, KCl and NH_4Cl.

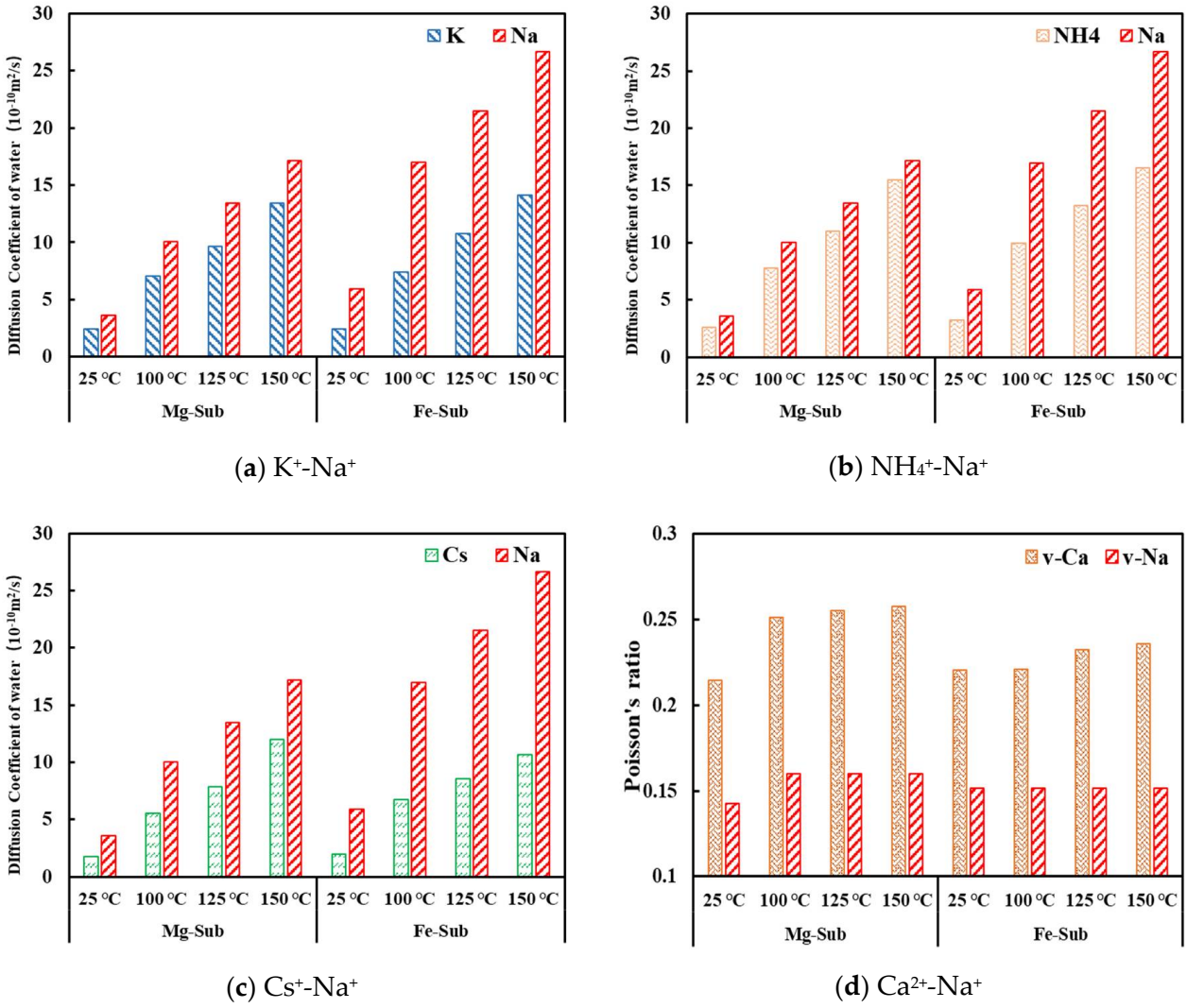

Figure 6. Diffusion coefficient of water of MMT system under different counterions and temperatures.

Figure 7 shows the relative concentration distribution of inhibitory cations and sodium ions in the Z-axis direction in the interlayer domain when saturated KCl and CsCl solutions are contained in the interlayer domain of the Mg-Sub-MMT system in mode 2, as well as the relative concentration distribution characteristics of sodium ions when no inhibitor is added (marked by Na-0 in the figure). The distribution peaks of K^+ and Cs^+ in the interlayer

domain are closer to the SiO_2 tetrahedral surface of montmorillonite crystal than those of Na^+. At the same time, compared with the original montmorillonite system without adding inhibitory ions, the main peak of Na^+ after addition is still near the middle of the interlayer domain, but the peak intensity is significantly lower than that of the original Na^+ (Na-0), indicating that Na^+ in the added system also has a tendency to transfer to the surface of the silica tetrahedron. This distribution indicates that when the inhibitory cations and sodium ions coexist in the interlayer domain, the inhibitory cations preferentially adsorb on the silica surface of the montmorillonite crystal layer, forming a more inner spherical coordination structure, thus inhibiting hydration and stabilizing the crystal layer structure. Moreover, Na^+ migrates to the surface, which further increases the ability of the cation to balance the negative charge in the crystal layer, reduces the electrostatic repulsion force and stabilizes the crystal layer structure.

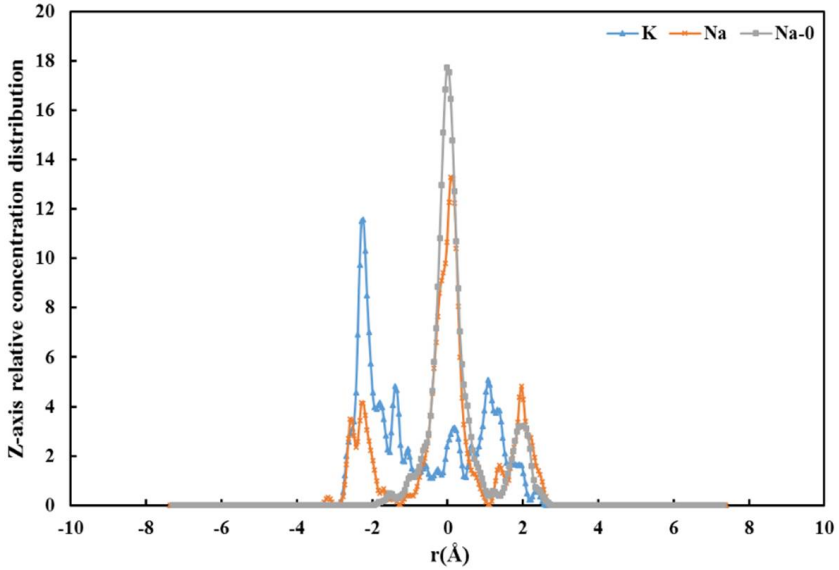

(**a**) K^+-Na^+

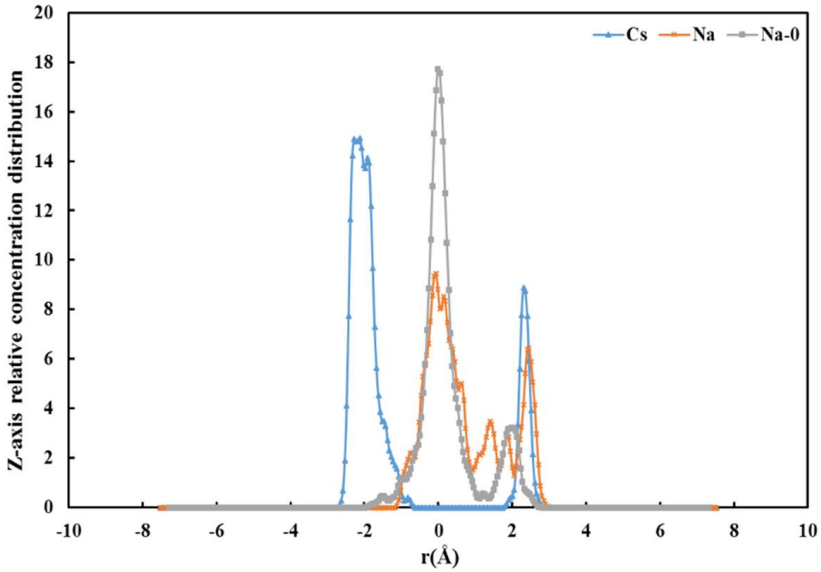

(**b**) Cs^+-Na^+

Figure 7. Z-axis relative concentration distribution of counterions.

The qualitative observation results of the relative concentration curve can be directly evaluated by the change in coordination number between cations and oxygen atoms on the surface of the montmorillonite silicon-oxygen tetrahedron (X-OB). Figure 8 shows the

change in coordination number between the inhibitory cations in the interlayer domain and sodium ions in the original system and oxygen atoms on the surface of montmorillonite silica under different temperature conditions. By comparison, it is found that the X-OB coordination number increases obviously after the addition of inhibitory cations, which indicates that the inhibitory cations tend to distribute on the clay surface and form more inner spherical ligands. The ability of the four kinds of inhibitory cations to form inner spherical ligands is $Cs^+ > K^+ > NH_4^+ > Ca^{2+}$, which also reflects the strength of the ability of the four kinds of cations to stabilize the crystal layer structure. At the same time, with the increase in temperature, the X-OB coordination number gradually decreases, which indicates that the increase in temperature weakens the immobilization of the inhibitory cations on the surface of the montmorillonite crystal layer, which is not conducive to the hydration inhibition effect of the cations.

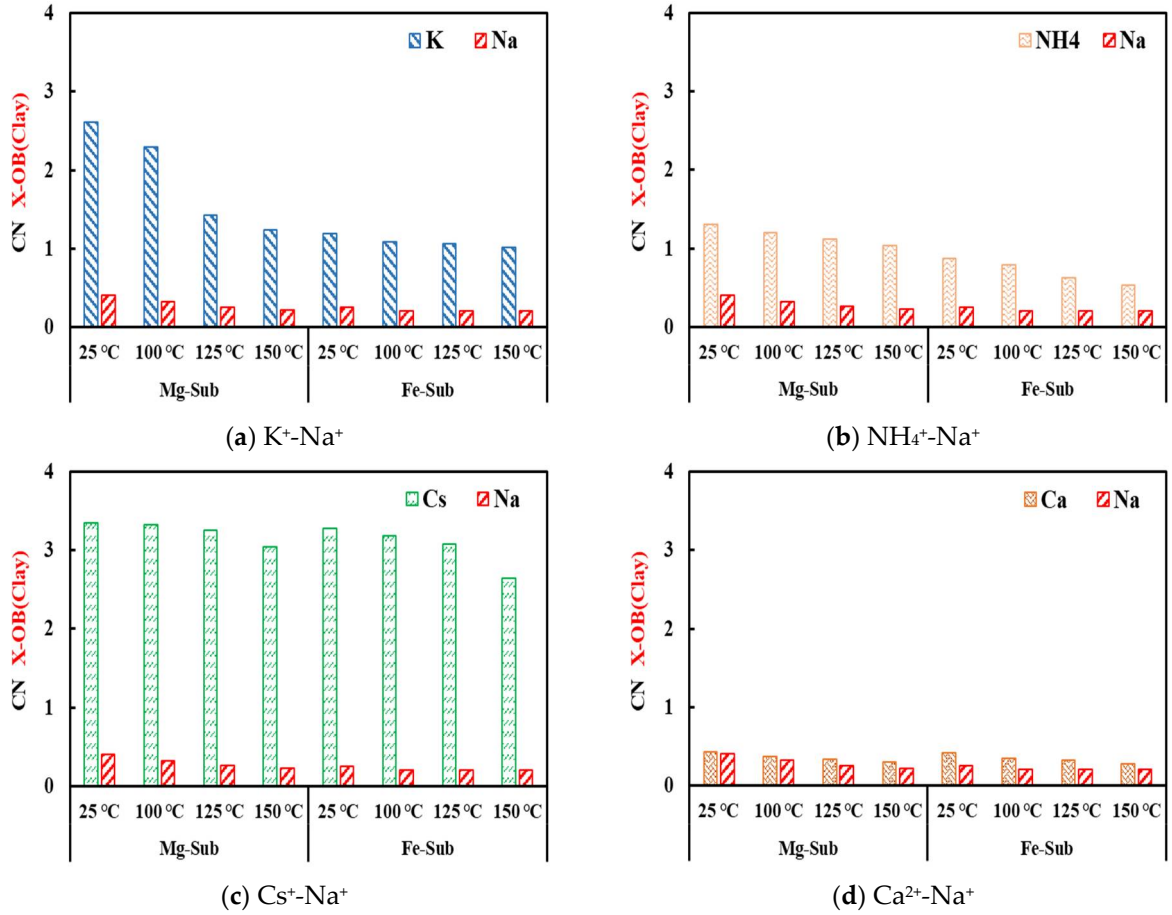

Figure 8. CN of counterions and O in silicon–oxygen tetrahedron surface under different counterions and temperatures.

When cations enter into the interlayer domain, another important evaluation criterion for their inhibition effect is their influence on the mechanical properties of montmorillonite crystals. Figures 9 and 10 show the changes in the mechanical properties of montmorillonite crystals after the entry of four kinds of inhibitory cations into the interlayer domain, focusing on the changes in the crystal stiffness (elastic modulus and Poisson's ratio).

In order to intuitively compare the ability of inhibiting cations to reduce the deterioration effect of mechanical properties of montmorillonite crystal under hydration, this section adds eight groups of mechanical properties under the same temperature and pressure conditions for two kinds of substitution models that have no water molecules in the interlayer, that is, mechanical properties under drying conditions. The reason for choosing to compare the mechanical properties of montmorillonite crystal without water in the interlayer domain is mainly to study whether the addition of inhibitory cations can strengthen

the montmorillonite crystal. This investigation allows determining whether the mechanical properties of the crystal with inhibitors are better than the original mechanical properties without water or to ensure that the deterioration degree of the mechanical properties of the crystal after hydration is weakened.

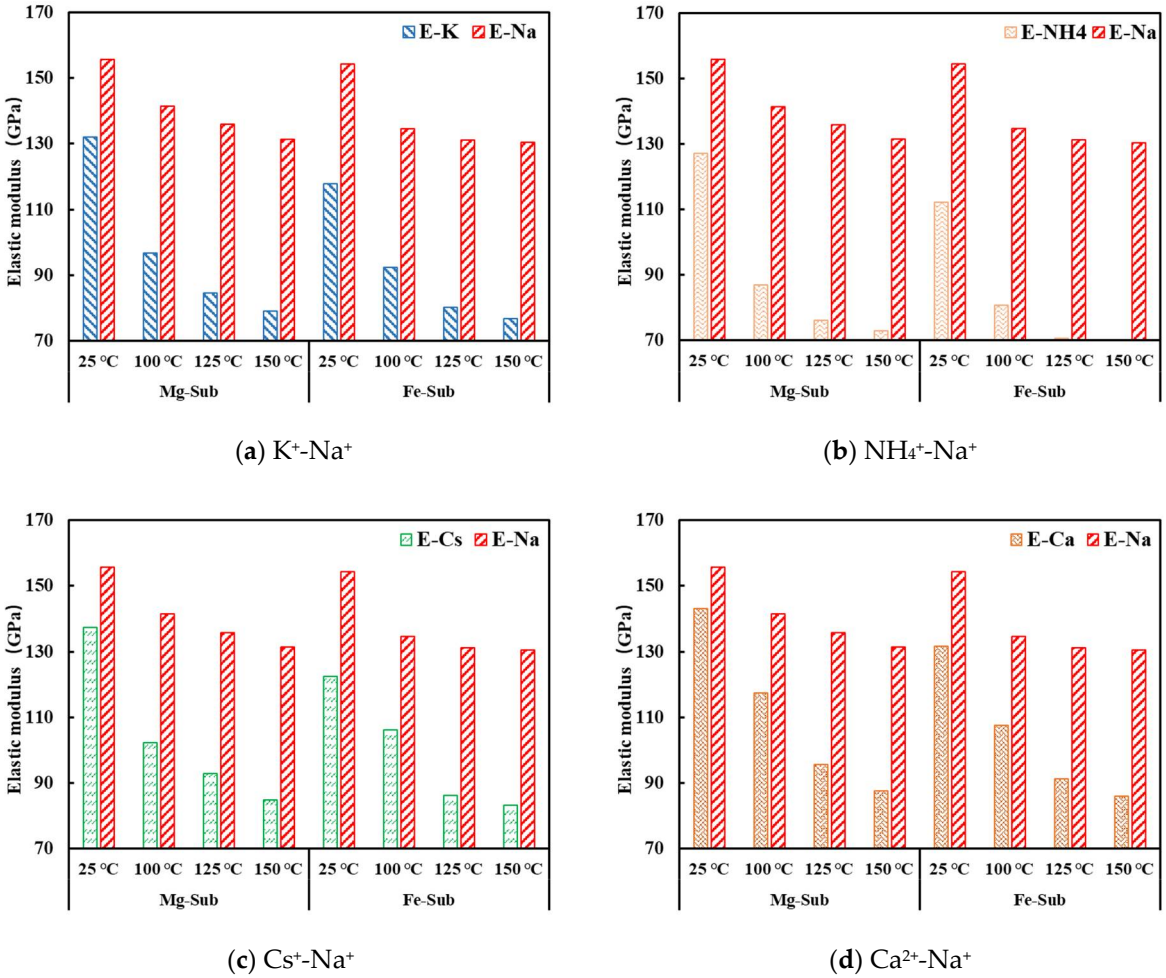

(**a**) K^+-Na^+ (**b**) NH_4^+-Na^+

(**c**) Cs^+-Na^+ (**d**) Ca^{2+}-Na^+

Figure 9. Elastic modulus of MMT crystals under different temperatures and inhibiting cations.

Firstly, the accuracy of the simulation results is verified by comparing the previous studies on the mechanical properties of montmorillonite crystals with inhibitory cations in the interlayer domain. The calculation results of bulk modulus and shear modulus of crystals with two layers of water molecules and saturated KCl, NH_4Cl and $CaCl_2$ in the interlayer domain by Professor Xu [17,35] are 69.16 GPa, 66.59 GPa and 67.83 GPa, 36 GPa, 34.58 GPa and 34.19 GPa respectively (the temperature, pressure and the number of water molecules are unknown). The elastic modulus and Poisson's ratio calculated based on isotropic assumption are 92.03 GPa, 88.43 GPa and 87.82 GPa, 0.278, 0.278 and 0.284, respectively. These values are similar to the simulation results (E, KCl: 75.76 GPa, NH_4Cl: 68.94 GPa, $CaCl_2$: 82.9 GPa; v, KCl: 0.260, NH_4Cl: 0.259, $CaCl_2$: 0.257) at 0.1 MPa and 25 °C in this paper. The slight difference may be caused by the difference in force field parameters, temperature and pressure conditions and the number of water molecules.

As shown in Figures 9 and 10, at different temperatures, the mechanical properties of montmorillonite crystals are still deteriorated when the saturated inhibitory salt solution is added in the interlayer compared with no water molecules in the interlayer, that is, when there is no hydration, indicating that the addition of inhibitory cations has no strengthening effect on the mechanical properties of montmorillonite crystals and can only reduce the deterioration degree of mechanical properties after hydration. At the same time, the degra-

dation degree increases with the increase in temperature, which indicates that temperature weakens the ability of cation to maintain the mechanical properties of crystal and reduces its inhibition effect. For example, in the Mg-Sub-MMT system with saturated KCl solution, the degradation degree of the crystal elastic modulus is 15.24% at 25 °C, but when the temperature rises to 150 °C, the degree of deterioration reaches 39.94%. This is consistent with the effect of temperature on the formation of the inner spherical coordination structure of inhibitory cations on the tetrahedral surface of montmorillonite crystal, both of which indicate that the inhibition of inhibitory cations will be weakened with the increase in temperature. The degradation degree of the mechanical properties of montmorillonite crystals under different temperatures is as follows: Ca^{2+} < Cs^{+} < K^{+} < $NH_4{}^{+}$. The average degradation degree of montmorillonite crystal in the Ca^{2+} system is only 27.46%, followed by 30.79% for Cs^{+}.

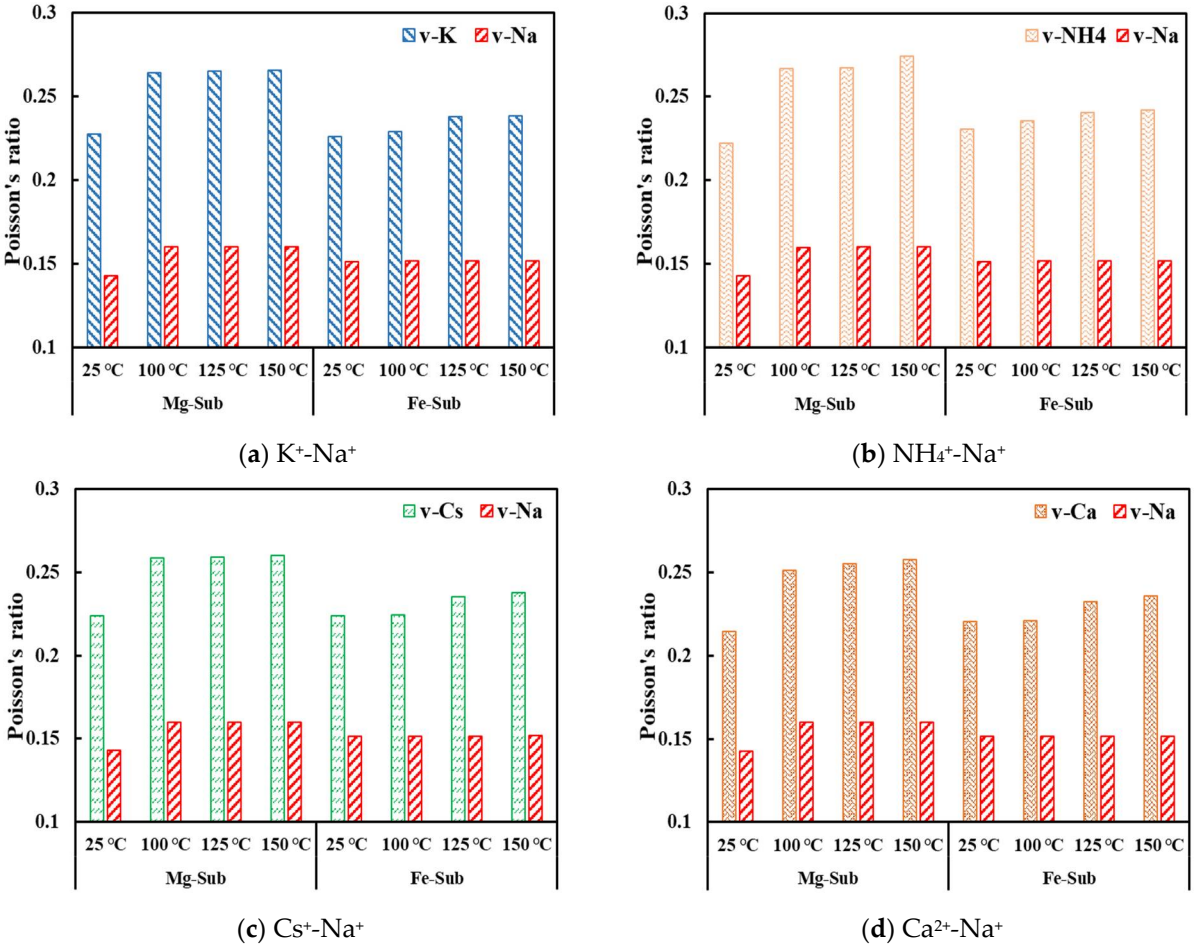

Figure 10. Poisson's ratio of MMT crystals under different temperatures and inhibiting cations.

Generally speaking, the temperature rise is not conducive to the inhibitory effect of the inhibitory cations in the montmorillonite system. The increase in temperature weakens the inhibition of cations on the hydration of montmorillonite by reducing the inhibitory effect of inhibitory cations on the diffusion of water molecules in the interlayer and the ability of cations to maintain the mechanical properties of the crystal.

4. Conclusions

In this paper, based on MD method, according to the characteristics of typical clay minerals contained in deep shale, combined with the types of inorganic salinization inhibitors commonly used in the field, the molecular dynamics models for micro inhibition evaluation of four typical cations (K^{+}, $NH_4{}^{+}$, Cs^{+} and Ca^{2+}) inhibiting clay hydration were

established. The molecular dynamics simulations of inhibiting hydration of clay minerals under different temperatures, pressures and types and concentrations of cation ions were carried out in order to explore the micro mechanism of the chemical inhibition effect of typical inorganic salt inhibitors on clay hydration and the temperature and pressure response characteristics. The following findings were obtained:

In terms of the micro mechanism of cations inhibiting clay hydration:

- The inhibitory cations (K^+, NH_4^+ and Cs^+) promote the contraction of clay interlayer spacing and compress the flow channel of ions and water molecules invading into the MMT interlayer.
- The inhibitory cations decrease the diffusivity of water and then weaken its ability to invade the formation.
- When the inhibitory cations (K^+, NH_4^+, Cs^+ and Ca^{2+}) are added into the interlayer domain, they will transfer to the surface of the crystal layer, resulting in the increase in coordination number with oxygen atoms on the silica surface of clay minerals, the improvement of the ability to balance the negative charge in the interlayer and the reduction in the electrostatic repulsion of the negative charge in the interlayer.

In terms of the characteristics of cationic clay hydration inhibition in response to temperature and pressure:

- The temperature rise is not conducive to the inhibitory effect of the inhibitory cations in the montmorillonite system. The increase in temperature weakens the inhibition of cations on the hydration of montmorillonite by reducing the inhibitory effect of inhibitory cations on the diffusion of water molecules in the interlayer and the ability of cations to maintain the mechanical properties of the crystal.
- The increase in pressure is helpful for the inhibitory cation to exert its inhibitory effect in the montmorillonite system. With the pressure rising, the inhibitory effect of cations on the montmorillonite hydration is enhanced by enhancing the inhibition of the water diffusivity in the interlayer and the ability of cations to maintain the mechanical properties of the crystal.
- The inhibitory properties of cations in different crystal lattices of substituted montmorillonites vary greatly. Generally, the cation inhibitory properties of Mg-Sub-MMT are better.

Author Contributions: Conceptualization, Y.Z.; methodology, Y.Z.; software, Y.Z.; validation, Y.Z. and C.X.; formal analysis, Y.Z. and C.X.; investigation, Y.Z.; resources, Y.Z. and C.X.; data curation, Y.Z.; writing—original draft preparation, Y.Z. and C.X.; writing—review and editing, Y.Z. and C.X. Both authors have read and agreed to the published version of the manuscript.

Funding: This research was funded by the National Natural Science Foundation of China (NSFC) (No. U19B6003-05) and Sinopec Ministry of Science and Technology Project (P18058-2).

Institutional Review Board Statement: Not applicable.

Informed Consent Statement: Not applicable.

Data Availability Statement: Data is contained within the article.

Acknowledgments: The authors are grateful for financial support to the National Natural Science Foundation of China (NSFC) (No. U19B6003-05) and Sinopec Ministry of Science and Technology Project (P18058-2).

Conflicts of Interest: The authors declare no conflict of interest.

References

1. Wilson, M.J.; Wilson, L. Clay mineralogy and shale instability: An alternative conceptual analysis. *Clay Miner.* **2014**, *49*, 127–145. [CrossRef]
2. Gui, J.; Ma, T.; Chen, P.; Yuan, H.; Guo, Z. Anisotropic Damage to Hard Brittle Shale with Stress and Hydration Coupling. *Energies* **2018**, *11*, 926. [CrossRef]

3. Gholami, R.; Elochukwu, H.; Fakhari, N.; Sarmadivaleh, M. A review on borehole instability in active shale formations: Interactions, mechanisms and inhibitors. *Earth Sci. Rev.* **2018**, *177*, 2–13. [CrossRef]
4. Luo, X.; Cui, M.; Zhang, X.; Yang, B. *Methods for Testing Shale Physics and Chemistry Properties*; State Bureau of Petroleum and Chemical Industry of China: Beijing, China, 2000.
5. Wang, G.; Ran, L.; Xu, J.; Wang, Y.; Ma, L.; Zhu, R.; Wei, J.; He, H.; Xi, Y.; Zhu, J. Technical development of charac-terization methods provides insights into clay mineral-water interactions: A comprehensive review. *Appl. Clay Sci.* **2021**, *206*, 106088. [CrossRef]
6. Skipper, N.T.; Chang, F.R.C.; Sposito, G. Monte Carlo Simulation of Interlayer Molecular Structure in Swelling Clay Minerals. 1. Methodology. *Clay. Clay Miner.* **1995**, *43*, 285–293. [CrossRef]
7. Skipper, N.T.; Chang, F.R.C.; Sposito, G. Monte Carlo Simulation of Interlayer Molecular Structure in Swelling Clay Minerals. 2. Monolayer Hydrates. *Clay. Clay Miner.* **1995**, *43*, 294–303. [CrossRef]
8. Chang, F.R.C.; Skipper, N.T.; Sposito, G. Computer Simulation of Interlayer Molecular Structure in Sodium Montmo-rillonite Hydrates. *Langmuir* **1995**, *11*, 2734–2741. [CrossRef]
9. Bains, A.S.; Boek, E.S.; Coveney, P.V.; Williams, S.J.; Akbar, M.V. Molecular Modelling of The Mechanism of Action of Organic Clay-Swelling Inhibitors. *Mol. Simul.* **2001**, *26*, 101–145. [CrossRef]
10. Park, S.-H.; Sposito, G. Monte Carlo Simulation of Total Radial Distribution Functions for Interlayer Water in Li-, Na-, and K-Montmorillonite Hydrates. *J. Phys. Chem. B* **2000**, *104*, 4642–4648. [CrossRef]
11. Sposito, G.; Park, S.H.; Sutton, R. Monte Carlo simulation of the total radial distribution function for interlayer water in sodium and potassium montmorillonites. *Clay. Clay Miner.* **1999**, *47*, 192–200. [CrossRef]
12. Greathouse, J.A.; Refson, A.K.; Sposito, G. Molecular Dynamics Simulation of Water Mobility in Magnesium-Smectite Hydrates. *J. Am. Chem. Soc.* **2000**, *122*, 11459–11464. [CrossRef]
13. Tinnacher, R.M.; Holmboe, M.; Tournassat, C.; Bourg, I.C.; Davis, J.A. Ion adsorption and diffusion in smectite: Mo-lecular, pore, and continuum scale views. *Geochim. Cosmochim. Acta* **2016**, *177*, 130–149. [CrossRef]
14. Lammers, L.N.; Bourg, I.C.; Okumura, M.; Kolluri, K.; Sposito, G.; Machida, M. Molecular dynamics simulations of cesium adsorption on illite nanoparticles. *J. Colloid Interface Sci.* **2017**, *490*, 608–620. [CrossRef]
15. de Pablo, L.; Chávez, M.L.; de Pablo, J.J. Stability of Na-, K-, and Ca-montmorillonite at high temperatures and pressures: A Monte Carlo simulation. *Langmuir* **2005**, *21*, 10874–10884. [CrossRef]
16. Miranda-Pascual, M.; Chávez-García, M. Monte Carlo molecular simulation of the Na-, Mg-, and mixtures of Na/Mg-montmorillonites systems, in function of the pressure. *Mol. Phys.* **2015**, *113*, 835–847. [CrossRef]
17. Xu, J.; Camara, M.; Liu, J.; Peng, L.; Zhang, R.; Ding, T. Molecular dynamics study of the swelling patterns of Na/Cs-, Na/Mg-montmorillonites and hydration of interlayer cations. *Mol. Simul.* **2017**, *43*, 575–589. [CrossRef]
18. Jin, W. Molecular Mechanics and Molecular Dynamics Simulation Studies of Interlayer Structure in Montmorillonites. Master's Thesis, Taiyuan University of Technology, Taiyuan, China, 2005.
19. Qing, Z. *Molecular Simulations of the Montmorillonite Interlayer microstructure and the Sorption towards Organics*; University of Chinese Academy of Sciences: Beijing, China, 2015.
20. Anderson, R.L.; Greenwel, H.C.; Suter, J.L.; Jarvis, R.M.; Coveney, P.V. Towards the design of new and improved drilling fluid additives using molecular dynamics simulations. *An. Acad. Bras. Ciênc.* **2010**, *82*, 43–60. [CrossRef] [PubMed]
21. Zhang, M.; Mao, H.; Jin, Z. Molecular dynamic study on structural and dynamic properties of water, counter-ions and poly-ethylene glycols in Na-montmorillonite interlayers. *Appl. Surf. Sci.* **2020**, *536*, 147700. [CrossRef]
22. Cygan, R.T.; Liang, J.J.; Kalinichev, A.G. Molecular Models of Hydroxide, Oxyhydroxide, and Clay Phases and the De-velopment of a General Force Field. *J. Phys. Chem. B.* **2004**, *108*, 1255–1266. [CrossRef]
23. Rappe, A.K.; Colwell, K.S.; Casewit, C.J. Application of a universal force field to metal complexes. *Inorg. Chem.* **1993**, *32*, 3438–3450. [CrossRef]
24. Rappe, A.K.; Casewit, C.J.; Colwell, K.S.; Goddard, W.A.; Skiff, W.M. UFF, a full periodic table force field for molecular mechanics and molecular dynamics simulations. *J. Am. Chem. Soc.* **1992**, *114*, 10024–10035. [CrossRef]
25. Casewit, C.J.; Colwell, K.S.; Rappe, A.K. Application of a universal force field to organic molecules. *J. Am. Chem. Soc.* **1992**, *114*, 10035–10046. [CrossRef]
26. Skipper, N.; Refson, K.; McConnell, J.D.C. Computer simulation of interlayer water in 2:1 clays. *J. Chem. Phys.* **1991**, *94*, 7434–7445. [CrossRef]
27. Boek, E.S.; Coveney, P.V.; Skipper, N.T. Monte Carlo Molecular Modeling Studies of Hydrated Li-, Na-, and K-Smectites: Understanding the Role of Potassium as a Clay Swelling Inhibitor. *J. Am. Chem. Soc.* **1995**, *117*, 12608–12617. [CrossRef]
28. Brindley, G.W.; Zalba, P.E.; Bethke, C.M. Hydrobiotite, a regular 1:1 interstratification of biotite and vermiculite layers. *Am. Mineral.* **1983**, *68*, 420–425.
29. Calvet, R. Hydratation de la montmorillonite et diffusion des cations compensateurs. *Ann. Agron.* **1973**, *11*, 257–268.
30. Zheng, Y.; Zaoui, A. How water and counterions diffuse into the hydrated montmorillonite. *Solid State Ion.* **2011**, *203*, 80–85. [CrossRef]
31. Chang, F.-R.C.; Skipper, N.T.; Sposito, G. Monte Carlo and Molecular Dynamics Simulations of Electrical Double-Layer Structure in Potassium−Montmorillonite Hydrates. *Langmuir* **1998**, *14*, 1201–1207. [CrossRef]

32. Posner, A.M.; Quirk, J.P. The adsorption of water from concentrated electrolyte solutions by montmo-rillonite and illite. *Proc. R. Soc.* **1964**, *278*, 35–56.
33. Lianfei, K. *Multi-Scale Study on the Basic Mechanisms of High Stress Mechanical Properties for Saturated Montmorillonite*; China University of Mining and Technology: Xuzhou, China, 2013.
34. Anderson, M.A.; Trouw, F.R.; Tam, C.N. Properties of water in calcium-and hexadecyltrimethylammonium-exchanged bentonite. *Clay. Clay Miner.* **1999**, *1*, 28–35. [CrossRef]
35. Hantal, G.; Brochard, L.; Laubie, H.; Ebrahimi, D.; Pellenq, R.J.-M.; Ulm, F.-J.; Coasne, B. Atomic-scale modelling of elastic and failure properties of clays. *Mol. Phys.* **2014**, *112*, 1294–1305. [CrossRef]